NOTICE

CERTAIN DATA CONTAINED IN THIS DOCUMENT MAY BE DIFFICULT TO READ IN MICROFICHE PRODUCTS.

Conf-9010292--2

Received by

JAN 22 1991

MEASUREMENTS OF GRAIN BOUNDARY PROPERTIES IN NANOCRYSTALLINE CERAMICS*

Y.-M. Chiang, I. P. Smyth, C. D. Terwilliger, W. T. Petuskey**, and J. A. Eastman†

Department of Materials Science and Engineering
Massachusetts Institute of Technology, Cambridge, MA 02139
**Department of Chemistry, Arizona State University, Tempe, AZ 85287
†Materials Science Division, Argonne National Laboratory, Argonne, IL 60439

CONF-9010292--2

DE91 006662

November 1990

The submitted manuscript has been authored by a contractor of the U.S. Government under contract No. W-31-109-ENG-38. Accordingly, the U.S. Government retains a nonexclusive, royalty-free license to publish or reproduce the published form of this contribution, or allow others to do so, for U.S. Government purposes.

DISCLAIMER

This report was prepared as an account of work sponsored by an agency of the United States Government. Neither the United States Government nor any agency thereof, nor any of their employees, makes any warranty, express or implied, or assumes any legal liability or responsibility for the accuracy, completeness, or usefulness of any information, apparatus, product, or process disclosed, or represents that its use would not infringe privately owned rights. Reference herein to any specific commercial product, process, or service by trade name, trademark, manufacturer, or otherwise does not necessarily constitute or imply its endorsement, recommendation, or favoring by the United States Government or any agency thereof. The views and opinions of authors expressed herein do not necessarily state or reflect those of the United States Government or any agency thereof.

Submitted to a special issue of *Acta Met.* Proceedings of the Conference on Materials with Ultrafine Microstructures, Atlantic City, NJ, October 1-5, 1990.

*Support from Office of Naval Research grant N00014-85-K-0645 for the SiC studies, NSF/MRL grant no. DMR-87-19217 for the Si and TiO_2 work, and an ONR Graduate Fellowship for CDT.

MASTER

DISTRIBUTION OF THIS DOCUMENT IS UNLIMITED

Submitted to a SPECIAL ISSUE OF ACTA MET. – PROC. OF THE CONFERENCE ON MATERIALS WITH ULTRAFINE MICROSTRUCT. ATLANTIC CITY, N.J. OCT. 1990.

MEASUREMENTS OF GRAIN BOUNDARY PROPERTIES IN NANOCRYSTALLINE CERAMICS

Y.-M. Chiang, I.P. Smyth, C.D. Terwilliger, W. T. Petuskey*, J.A. Eastman†

Department of Materials Science and Engineering
Massachusetts Institute of Technology, Cambridge, MA 02139
*Department of Chemistry, Arizona State University, Tempe, AZ 85287
†Argonne National Laboratory, Argonne, IL 60439

Introduction

The advent of nanocrystalline ceramics prepared by a variety of solution-chemical and vapor deposition methods offers a unique opportunity for the determination of grain boundary properties by "bulk" thermodynamic methods. In this paper we discuss results from two types of measurements on model nanocrystalline ceramics.

The first is a solution thermodynamic measurement of the activity of nanocrystalline SiC in polycarbosilane-derived silicon carbide fibers (Nicalon®). This material is a commercially available nanocrystalline ceramic, originated by Yajima et al. [1-2], and now produced in yarn form by Nippon Carbon Company for use as a reinforcement in ceramic and metal matrix composites. In the so-called "ceramic" grade it has a fiber diameter of ~10 μm, a grain diameter of ~2 nm and the approximate composition Si_3C_4O. Structural studies have shown that Nicalon consists of well-ordered cubic (β or 3C polytype) SiC grains separated by a very thin grain boundary layer (<1 nm thick) containing the oxygen [3]. The physical properties and chemical reactivity of these fibers are distinctly different from that of bulk silicon carbide [4]. In particular, Nicalon is known to react with oxide composite matrices to form a thin (20-50 nm) carbon interfacial layer that is essential for fiber-matrix debonding and the achievement of high fracture toughness [5]. This reaction has been modeled as the oxidation of SiC by Cooper and Chyung [6] and Benson et al. [7]. Both groups have assumed that the SiC is in its standard state. We believe that this assumption is seriously in error due to the nanocrystalline nature of the fiber. There is experimental evidence that the thermodynamic and/or kinetic behavior of Nicalon is unique; the beneficial interfacial reaction does not take place in the case of single crystal SiC whiskers [5]. A more complete analysis must therefore take into account the greater driving force in nanocrystalline SiC, as well as possible differences in kinetics. We have attempted to measure the excess free energy of the nanocrystalline form relative to a reference of recrystallized SiC by equilibrating samples with an Al-Si melt at fixed carbon activity (pinned by Al_4C_3 formation). Direct measurement of the alloy composition and analysis of the microstructure has allowed the dissolution reaction to be identified and a lower limit for the SiC activity in the nanocrystalline form to be determined.

A second method of measuring grain boundary properties we have investigated for nanocrystalline Si and TiO_2 is high temperature calorimetry. In appropriate samples the grain boundary enthalpy can be measured through the heat evolved during grain growth. Preliminary results on nanocrystalline Si prepared by the recrystallization of amorphous evaporated films and on TiO_2 condensed from the vapor phase are discussed.

Measurement of Silicon Carbide Activity in Nanocrystalline Nicalon Fibers

We characterized the excess Gibbs free energy of the nanocrystalline SiC in Nicalon relative to the "bulk" 3C polytype, using a solution thermodynamic method first used by Chipman [8-10] to measure the free energy of formation of silicon carbide, and more recently by Sambasivan et al. [11] for determining the difference in free energy of 6H and 3C silicon carbide polytypes. In this method the silicon carbide of interest is equilibrated with an alloy of silicon that acts as a "silicon potentiometer." The silicon activity of the sample is determined by measuring the alloy concentration after equilibration, using known activity-concentration relationships for the alloy. Since it is advantageous to use an alloy in which the Si concentration is high enough for accurate measurement, yet low-melting enough to avoid grain coarsening during the experiment (T<1000°C), we used Al-Si alloys instead of the Fe and Pb alloys of Chipman et al. [8-10] or the Au-Si alloys of Sambasivan et al. [11]. The results may also be pertinent to metal matrix composites in which Nicalon fibers are used to reinforce aluminum alloy matrices.

A schematic of the experimental configuration is shown in Fig. 1. A molten Al-Si alloy was used to infiltrate the samples in an apparatus constructed of graphite. Reaction between the graphite and the alloy

forms Al_4C_3, leading to a three-phase assemblage (SiC-Al_4C_3-liquid alloy). If equilibrium between all three phases is achieved, the reaction of interest is:

$$3SiC + 4\underline{Al} \rightarrow 3\underline{Si} + Al_4C_3 \qquad K = a_{Si}^3 a_{Al4C3}/a_{SiC}^3 a_{Al}^4 \qquad (1)$$

where the activities of Al and Si are determined by the analysis of the alloy concentration and Al_4C_3 is assumed to be of unit activity. In reactions between Al-Si alloys and carbon, Al_4C_3 is found to form rapidly at the interface [12]. From the a_{Si} values for the alloys in equilibrium with nanocrystalline and reference SiC samples, it is then possible to determine the activity of the nanocrystalline phase $a_{SiC(n)}$ relative to the reference (standard state, $a_{SiC} = 1$), as well as their respective formation free energies.

Standards were prepared using graphite crucibles with 1/4" bore, into which alloys were infiltrated at 700°C with a 1/4" graphite rod in a resistance heated vacuum furnace. We attempted to use vapor-liquid-solid (VLS) grown SiC whiskers [13] and sintered α-SiC as standards, but these failed to reach equilibrium (too low a Si concentration). A successful standard containing the necessary three-phase SiC-Al_4C_3-liquid alloy equilibrium was instead prepared by reacting carbon fibers [14] with an Al-9.5% Si melt. Copious amounts of Al_4C_3 were formed in this reaction, enriching the alloy in Si to the 11.5% level at equilibrium. For the Nicalon containing samples, a cylindrical billet (1"x6") was fabricated by pressure infiltration using the Experimental Rig for the Infiltration of Composites [15] at MIT. Chopped fibers (NC200 grade) of 1/4-1/2" length, cleaned of their vinyl acetate sizing by firing in air at 375°C for 4 h., were packed to about 20 vol% density in a graphite foil-lined high-purity Al_2O_3 crucible. A perforated graphite spacer separated the starting alloy (~12% Si) [16] from the fibers. After evacuation the fibers were infiltrated with the molten alloy at 700°C by applying an argon pressure of 800 psi, over a period of ~30 min. The cooled sample was then sectioned for subsequent annealing experiments, for which graphite foil containers were used. All anneals were conducted in flowing argon at 1050K, and samples were rapidly quenched from the hot zone into room temperature water.

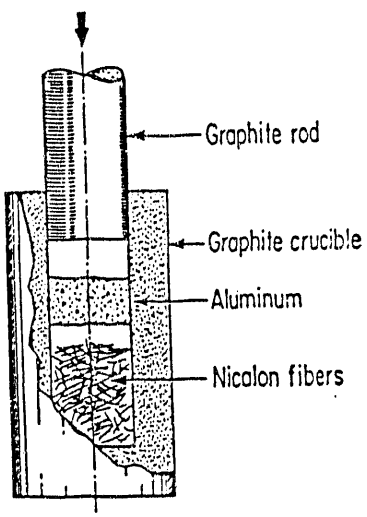

Figure 1. Experimental apparatus for infiltration and equilibration of SiC samples with Al-Si alloy.

For microstructural observations and composition analysis by electron microprobe [17] (EPMA) the samples were polished to a 1 μm finish with diamond compound. In the EPMA analysis, 32x32 μm rastered areas were analyzed to determine the Al and Si concentrations of alloy regions well away from SiC and Al_4C_3 particles. The raster size is well above the smaller-scale inhomogeneities caused by phase separation during cooling. Ten areas of this size were analyzed in each sample, and the cumulative results were used to determine the alloy composition. Al and Si metals were used as the calibration standards. Individual phase compositions were measured using ~1 μm diameter spot analyses. SiC and SiO_2 were used as the composition standards for C and O respectively.

Table I shows the free energy of SiC formation at 1050K obtained from this standard, compared with available literature values. There is especially good agreement with the Janaf Table value [18] and the data of Sambasivan et al. [11]. In the case of the Nicalon^R fibers, a clearly higher Si concentration in the alloy was observed at all annealing times compared to the standard, as shown in Fig. 2. This alone indicates a higher activity of the SiC phase. The error bars shown reflect the standard deviation of the ten rastered areas measured, and are therefore conservative (for example the X-ray counting statistics error of the cumulative measurement is negligible on this scale). However, microstructural analyses indicated that equilibrium was not achieved during this experiment. Instead of simple dissolution to the equilibrium alloy concentration, a *metastable* Si crystalline phase appeared (Fig. 3). These samples lie in a compatibility field of the Si-Al-C ternary phase diagram where solid Si is not an equilibrium phase at this temperature [21,22]. The Si phase appeared to grow out from the fiber-melt interface (Fig. 3), for annealing times of up to 4 h. Quenching studies showed that these crystals are not formed upon cooling. Al_4C_3 particles were found in the interfacial region during this stage of the reaction.

Table I. Free Energies of Formation for β-SiC at 1050K.

Reference	ΔH_f (kJ/mol)	ΔS_f (J/mol K)	ΔG_f (kJ/mol)
JANAF Tables [18]	-72.3	-7.2	-64.8
Laptev et al. [19]	-64.9	-7.3	-57.2
Grieveson et al.[20]	-63.0	-8.1	-54.5
Sambasivan et al. [11]	-81.0	-15.1	-65.1
This work			-69.7

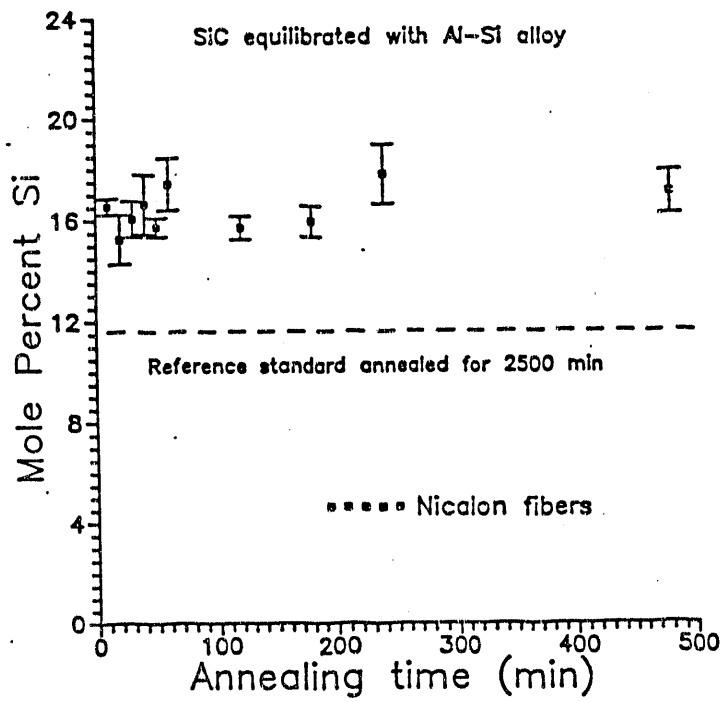

Figure 2. Silicon concentration in the Al-Si alloy in contact with Nicalon fibers.

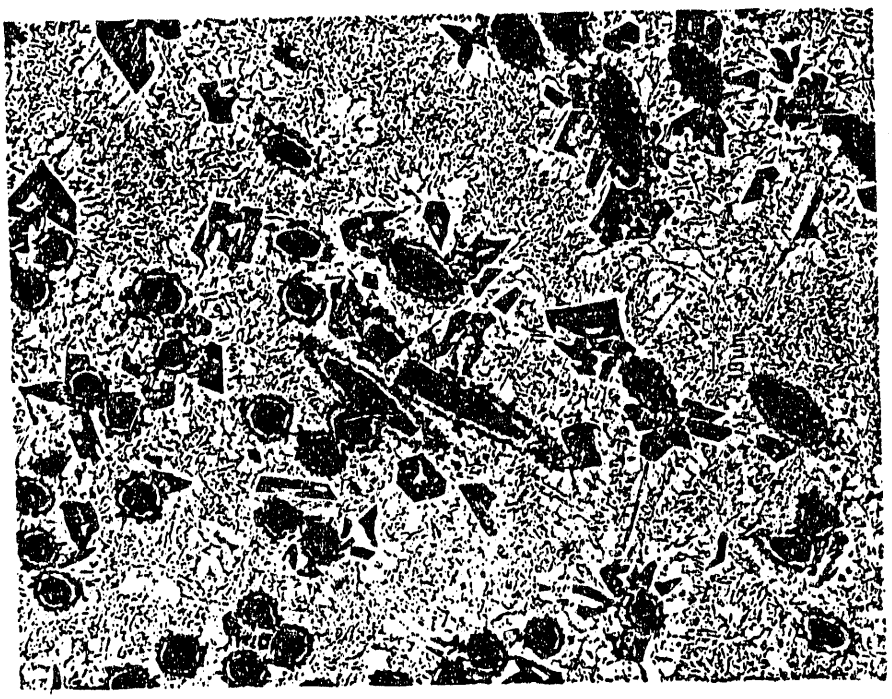

Figure 3. Nicalon fibers dissolving in Al-Si alloy, showing angular particles of metastable Si phase.

As a result, the values in Fig. 2 cannot be taken to be the Si concentration in equilibrium with Nicalon. We can rewrite equation (1) to show the formation of metastable Si upon dissolution of Nicalon:

$$3SiC(Nicalon) + 4\underline{Al} \rightarrow 3Si(solid) + Al_4C_3 \qquad (2)$$

This dissolution reaction continued for annealing times up to 4 h. Beyond 4 h., however, the metastable Si phase was consumed, and recrystallized β-SiC was evident in EPMA analysis (not shown). This shows that the reaction in (2) moves back towards the left when recrystallized equilibrium β-SiC forms. Due to the absence of equilibration, the Nicalon activity cannot be unequivocally established. It is, however, possible to obtain a lower limit for the activity based on the observation that equation (2) does proceed to the right in this experiment. Equation (2) is the sum of the following reactions:

$$3SiC(Nicalon) \rightarrow 3Si(solid) + 3\underline{C} \qquad \Delta G_1 = +\ 193{,}909\ J/mole + RT\ \ln(a_C{}^3/a_{SiC(N)}{}^3) \qquad (3)$$

$$3\underline{C} + 4\underline{Al} \rightarrow Al_4C_3 \qquad \Delta G_2 = -\ 160{,}356\ J/mole - RT\ \ln a_C{}^3 a_{Al}{}^4 \qquad (4)$$

where the numerical values are standard free energies of formation for SiC and Al_4C_3 [18]. The standard states are solid β-SiC, solid Si, and solid Al_4C_3 respectively. The activity of Si is taken to be unity given the appearance of crystalline Si. The activity of carbon in solution (a_C) is assumed to be the same for both equations 3 and 4; that is, local equilibrium of carbon with both the dissolving SiC and the recrystallized Al_4C_3 is assumed. This is likely to be the case given the close physical proximity of the two phases and the rapid diffusion of carbon in the alloy melt. The activity of $\underline{Al}$ is the experimentally measured value (X_{Al}=0.835, at which a_{Al}=0.80 using activity coefficients for Al-Si melts from ref. 23). For reaction (2) to proceed to the right, its free energy must be more negative than the sum of those for reactions (3) and (4):

$$\Delta G_2 < \Delta G_1 + \Delta G_2 = 33{,}553\ J/mol - RT\ \ln a_{Al}{}^4 a_{SiC(n)}{}^3,$$

from which we obtain a lower limit for the activity and excess free energy of Nicalon^R SiC:

$$a_{SiC(n)} > 4.6\ ; \qquad \Delta G_{excess}(Nicalon^R) > 13.9\ kJ/mol.$$

We can compare this value to the excess free energy attributable to grain boundaries:

$$\Delta G_{gb} = 3\gamma V_m/2r$$

where γ is the specific grain boundary energy, V_m the molar volume of SiC (12.1 cm^3/mol) and r the grain radius (0.85 nm as determined by X-ray line broadening and TEM [7]). For a reasonable value of the grain boundary energy (~1 J/m^2), ΔG_{gb} would be 21 kJ/mole. The measured lower limit for ΔG_{excess} appears quite reasonable by comparison. Notice that this excess energy is a large fraction (>20%) of the free energy of formation for our reference β-SiC (Table I), confirming the fact that Nicalon is not accurately represented thermodynamically by "phase pure" SiC, and that the higher activity should be taken into account when the reactivity of Nicalon fibers is considered.

Calorimetric Measurement of Grain Boundary Enthalpy during Grain Growth

Although grain boundary and surface energies are important parameters for quantifying the driving force in almost all microstructure development problems, accurate values are not available for any ceramic system. Indirect methods such as the measurement of dihedral angles have proved problematic due to surface facetting [24], and in any case can only yield relative energies. Calorimetry during grain growth is one of the few direct methods for the measurement of grain boundary energies. The heat evolved is a direct measure of grain boundary enthalpy if no other processes are occurring simultaneously in the material. (To obtain the free energy, the grain boundary entropy must of course be separately determined.) It appears that the first attempt to use this method was made in 1956 by Astrom [25], who reported a grain boundary enthalpy for zinc. Special efforts were made in the design of a calorimeter to detect the extremely small amount of heat released during growth from an initial grain size of 10 μm to a final grain size of 1 mm, but nevertheless, the accuracy of the experiment was poor. More recently available processes for fabricating ultrafine-grained materials [26] with correspondingly large grain boundary surface areas (~10^8 m^2/m^3) have made this method much more feasible, as demonstrated by Chen et al. [27] in microcrystalline metal alloys. Here we report preliminary results for higher temperature ceramic systems.

Two types of samples (Si and TiO_2) were examined. Nanocrystalline Si was formed by crystallizing electron-beam evaporated amorphous silicon films (0.75 μm thick). Between 1.3-1.5 mg of the resulting flakes were used as DSC specimens. Crystallization and grain growth were conducted in the scanning mode (90°/min) in the high temperature differential scanning calorimeter (Netzsch DSC 404) using alumina crucibles under an atmosphere of flowing argon. Runs conducted with laboratory grade argon, ultra-high

purity (UHP) argon, and UHP argon passed over a heated titanium getter showed that thermal artifacts due to oxidation of the silicon were absent. Baseline and calibration runs were first conducted by measuring the heat capacity of a sapphire disc as a function of temperature and comparing with literature values. Transmission electron microscopy (JEOL 200CX and Akashi EM-002B) was used to examine the grain structure before and after grain growth. Flakes of nanocrystalline TiO_2 (~200 μm thick) made by the inert gas condensation process [28] were also examined. The as-received (black) TiO_2 flakes were first oxidized in air at 350°C for 48 h., followed by 117 hours at 450°C. These temperatures are well below those at which grain growth has been reported in this system [28-29]. After oxidation the flakes retained a few visible gray specks that may indicate locallized regions that were still reduced. Grain growth was conducted inside alumina crucibles in the calorimeter under static air, with a scanning rate of 50°/min.

The DSC output for a scanning run of amorphous silicon is shown in Fig. 4. At this scanning rate, crystallization begins at 759°C and peaks at 795°C. Electron diffraction confirmed that the silicon is polycrystalline, and a microstructure with two grain size populations could be imaged in TEM. There is a population of anomalously large grains 30-100 nm in diameter occupying approximately 20% of the material by volume. Rather than acting as "seed" grains for discontinuous grain growth, it appeared that the size of these grains remained static during the DSC experiment. There was a "matrix" of much finer grains on the order of 5 nm in size, which do coarsen during the DSC experiment, to a final grain size of ~20 nm. However, many grains are not clearly resolvable even after grain growth, and this estimate of the "average" grain size may be in error by as much as a factor of two. The exothermic event in the DSC output beginning at 932°C has the shape one would expect for a non-isothermal grain growth process [34-35]. The total enthalpy of this event is -215 J/g (-6039 J/mole), which for initial and final grain sizes of 5 and 20 nm respectively yields a grain boundary enthalpy of ~0.6 J/m^2, assuming spherical grains. While this is not an unreasonable value, it is clear that more accurate measurements of the grain boundary enthalpy will require a more well-characterized and uniform microstructure.

The DSC output for nanocrystalline TiO_2 (n-TiO_2) is shown in Fig. 5. A clear exothermic departure from the baseline can be seen at 600°C. We attribute this to grain growth since previous studies have found that grain growth begins in n-TiO_2 above 550°C [36-37]. Grain size measurements have not yet been made on these specific samples, but other TiO_2 samples made by this method typically show a grain size of 12 nm. Assuming this to be the initial grain size and a final grain size that is much larger, the total enthalpy of the grain growth exotherm (-10.26 kJ/mole) corresponds to a specific grain boundary enthalpy of ~1.1 J/m^2 assuming spherical grains, which is quite reasonable. Here as in the case of the silicon samples, more accurate measurements will require a full characterization of the initial and final grain structures.

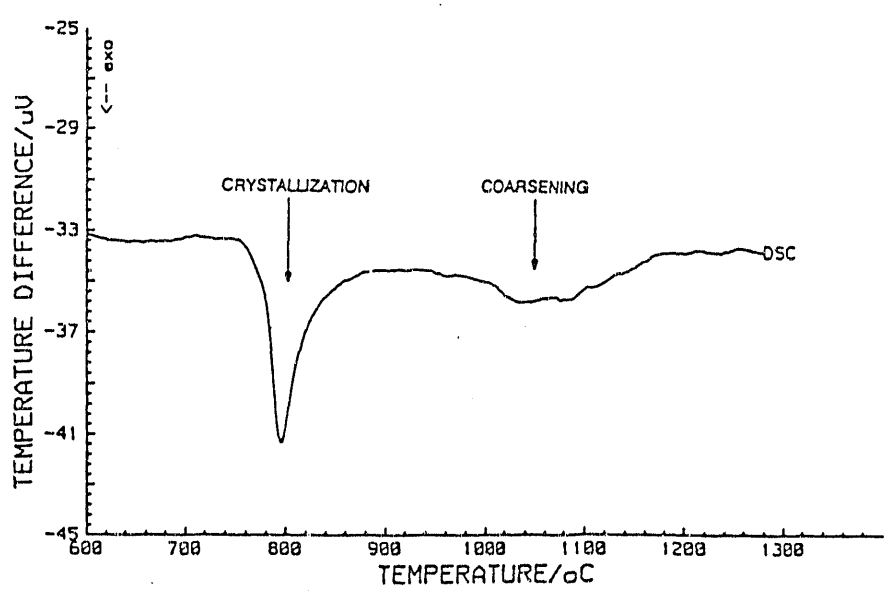

Figure 4. DSC output for crystallization and coarsening of amorphous silicon.

These initial results demonstrate that thermal analysis of nanocrystalline ceramics is feasible, and in particular that the evolved enthalpies are well within the measurement sensitivity of current high temperature calorimeters. The experiments to date also illustrate the areas of difficulty. Characterization of the initial microstructure (initial grain boundary area) is perhaps the most important step. This is clearly facilitated by uniform microstructures. If the initial grain size, shape, and size distribution can be measured accurately, correspondingly accurate values for the specific grain boundary enthalpy can be obtained.

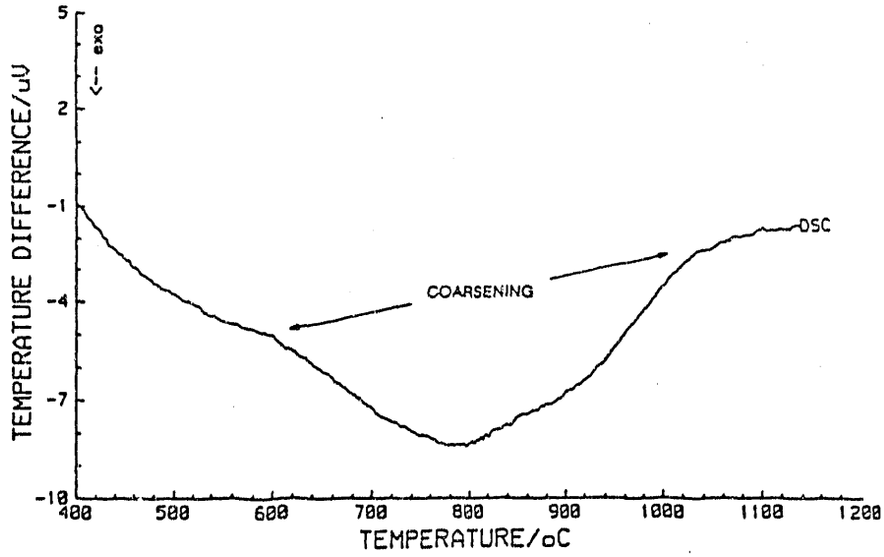

Figure 5. DSC output during grain growth of nanocrystalline TiO_2.

Acknowledgements

Support from Office of Naval Research grant N00014-85-K-0645 for the SiC studies, NSF/MRL grant no. DMR-87-19217 for the Si and TiO_2 work, and an ONR Graduate Fellowship for CDT are gratefully acknowledged. We thank D. Lange, J.A. Isaacs, and M. Frongillo for experimental assistance, D.H. Carter for providing the VLS whiskers, and A. Mortensen for useful discussions.

References

1. S. Yajima, J. Hayashi, M. Omori and K. Okamura, *Nature* 261, 683 (1976).
2. S. Yajima, K. Okamura, J. Hayashi and M. Omori, *J. Am. Cer. Soc.* 59[7-8], 324 (1976).
3. C. Laffon, A. Flank, P. Lagarde, M. Laridjani, R. Hagege, P. Olry, J. Cotteret, J. Dixmier, J. Miquel, H. Hommel and A. Legrand, *J. Mat. Sci.* 24, 1503 (1989).
4. G. Simon and A. Bunsell, *J. Mat. Sci.* 19, 3649 (1984).
5. J.J.Brennan, p. 549 in Tailoring Multiphase and Composite Ceramics, *Mat. Sci. Res., Vol. 20*, Plenum Press, New York, (1986); and United Technologies Research Center report R85-916777-2, May 1985.
6. R.F. Cooper and K. Chyung, *J. Mat. Sci.* 22, 3148 (1987).
7. P.M. Benson, K.E. Spear and C.G. Pantano, *Ceram. Eng. Sci. Proc.* 9[7-8], 663 (1988).
8. D.H. Kirkwood and J. Chipman, *J. Phys. Chem.* 65[6], 1082 (1961).
9. R.H. Rein and J. Chipman, *J. Phys. Chem.* 67[4], 839 (1963).
10. J. Chipman, J.C. Fulton, N. Gokcen and G.R. Caskey, Jr., *Acta. Met.* 2[3], 439 (1954).
11. S. Sambasivan, C. Capobianco and W.T. Petuskey, to appear in *J. Am. Cer. Soc.*
12. Y.-M. Chiang, R.F. Messner, C.D. Terwilliger and D. Behrendt, to appear in *Mat. Sci. and Eng. B.*
13. J.V. Milewski, F.D. Gac, J.J. Petrovic and S.R. Skaggs, *J. Mat. Sci.* 20, 1160 (1985).
14. P55 fibers, Union Carbide Corporation.
15. P.A.C. Roudier, M.S. Thesis, MIT, Sept. 1989.
16. Provided by M. G. Chu, Alcoa Laboratories, Alcoa Center, PA.
17. Cameca MBX electron microprobe, equipped with Tracor-Northern TN-1310 WDS system.
18. JANAF Thermochemical Tables, U.S. Dept. of Commerce, NBS, 2nd Edition (1971).
19. D.M. Laptev, V.V. Vasilev, V.G. Mizin, G.V. Serovand and M.S. Khurushchev, *Steel USSR*, 5, 467 (1975).
20. P. Grieveson and C.B. Alcock, Special Ceramics, *Proc. Brit. Ceram. Research Assoc.*, 1, 183 (1959).
21. C.A. Handwerker, M.D. Vaudin, U.R. Kattner and D.-J. Lee, *Acta Met.*, Proc. on Metal-Ceramic Interfaces, edited by M. Ruhle and A.G. Evans.
22. R. Warren and C.-H. Andersson, *Composites* 15, 101 (1984).
23. Z. Kozuka, S. Yasugi, W. Nakajima and J. Moriyama, *Denki Kagaku* 34, 35 (1966).
24. C.A. Handwerker, Sc.D. Thesis, Massachusetts Institute of Technology, 1983.
25. H.U. Astrom, *Acta Met.* 4, 562 (1956).
26. L.E. Brus, R.W. Siegel, et al., *J. Mater. Res.* 4, 704 (1989).
27. L.C. Chen and F. Spaepen, *Nature* 336, 366 (1988); *Acta Met.*, this issue; and to appear in *J.Appl.Phys.*
28. R.W. Siegel, S. Ramasamy et al., *J. Mater. Res.* 3, 1367 (1988).
29. H. Hahn, J. Logas, and R.S. Averback, *J. Mater. Res.* 5, 609 (1990).

END

DATE FILMED

02 / 11 / 91